Chapter 2
Fundamentals of Photophysics, Photochemistry, and Photobiology

Ulrich E. Steiner

Abstract This chapter provides an introduction to the photophysical and photochemical fundamentals that should represent a useful scientific background for applicants of photodynamic therapy (The references given in the abstract provide some access to generally recommended textbooks or reviews of the various areas.). First, the absorption of light and the basics of spectrophotometry (Parson in Modern Optical Spectroscopy. With exercises and examples from biophysics and biochemistry. Springer-Verlag, Berlin Heidelberg, 2007; Burgess and Frost in Standards and best practice in absorption spectrometry. Blackwell Science, London, 1999; Gore in Spectrophotometry and Spectrofluorimetry. Oxford University Press, Oxford, 2000) are dealt with, including a theoretical background to understand absorption spectra. Then follows a survey of photophysical processes with the characteristic pathways of radiationless and radiative decay of electronically excited states (Lakowicz in Principles of fluorescence spectroscopy. Springer Science+Business Media, New York, 2006), electronic energy transfer and a brief introduction into singlet oxygen (Schweitzer and Schmidt, Chem Rev 103:1685–1757, 2003). The photochemistry part (Turro et al. in Principles of molecular photochemistry: an introduction. University Science Books, Sausalito, 2009; Klán and Wirz in Photochemistry of organic compounds. From concept to practice. Wiley, Chichester, 2009; Stochel et al. in Bioinorganic Photochemistry, Wiley, Chichester, 2009) explains the concept of photoreactions as excited state chemistry and changes of chemical properties and chemical reactivity as a consequence of the modified electronic structure in the excited state. Elementary processes dealt with comprise photoinduced electron transfer (Kavarnos in Fundamentals of photoinduced electron transfer. VCH Publishers, New York, 1993), excited state proton transfer and *cis/trans*-photoisomerization. Photobiological aspects, such as photosynthesis and vision (Kohen et al. in Photobiology.

U. E. Steiner (✉)
Department of Chemistry, University of Konstanz, D-78457 Konstanz, Germany
e-mail: ulrich.steiner@uni-konstanz.de

M. H. Abdel-Kader (ed.), *Photodynamic Therapy*,
DOI: 10.1007/978-3-642-39629-8_2,

Academic Press, San Diego, 1995; Batschauer in Photoreceptors and Light Signaling. Comprehensive Series in Photochemical and Photobiological Sciences. The Royal Society of Chemistry, Cambridge, 2003), are briefly outlined.

2.1 Photophysics

2.1.1 Light and Color

Their specific colors are one of the important sensory properties of chemical compounds. In nature, the green of leaves, the yellow, red and blue of flowers, and the red of blood are prominent indicators of chlorophyll, flavonoids, anthocyanins, and hemoglobin, respectively. What our vision senses as uniform, single colors, is usually the impression of light that can still be decomposed into a spectral continuum of colors by the optical effect of dispersion exhibited by a prism or a grating. Spectrally pure light is characterized as electromagnetic radiation of a definite wavelength λ. The range of wavelengths from about 400 nm to about 750 nm represents the visible part of the electromagnetic spectrum (Fig. 2.1), that extends from the region of γ-rays at the short wavelength end to the region of radio waves at the long wavelength end.

The characteristic color of a chemical compound is due to its characteristic absorption of parts of the visible spectrum from the ambient white light. The remaining transmitted or remitted spectral mixture of light determines the color

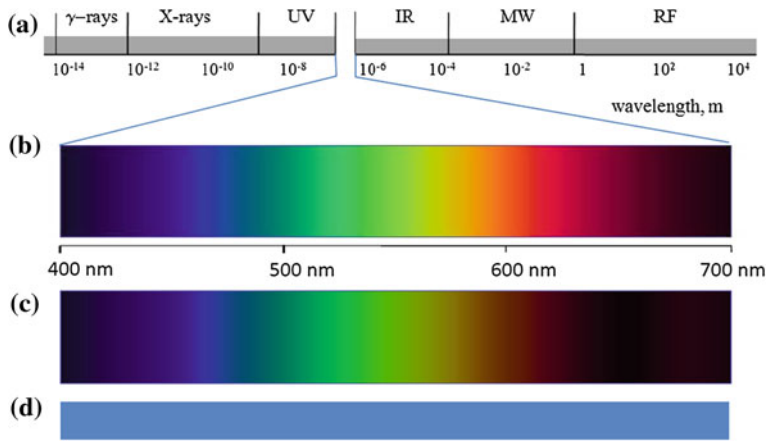

Fig. 2.1 **a** Regions of the electromagnetic spectrum and localization of the UV/vis range, **b** colors of the visible spectrum of a white light source, **c** colors of the visible spectrum after transmission through a solution of methylene *blue*, **d** perceived color of the methylene *blue* solution

that we see. However, it is the spectral characteristics of the *absorbed* light that carries the essential information on the electronic structure of the molecules and their concentration if we are dealing with dilute systems such as solutions. Quantitative measurements of the absorption characteristics in the UV to near infrared define the realm of UV/vis spectrophotometry or, in another term relating to the underlying physical process: electronic absorption spectroscopy.

2.1.2 Spectrophotometry

The most convenient way to measure the absorption characteristics of a chemical compound is by employing a homogenous transparent solution in some solvent [1–3]. If the solution is dilute, it is usually justified to assume that the absorption characteristics are determined by the individual solute molecules. In a spectrophotometer, the transmission of light through a sample cuvette is measured as a continuous function of the wavelength. For relating the observed transmission to the absorption of the solute molecules it is important to eliminate any light attenuation effect due to the cuvette windows and the solvent. Such effects are due to reflection of some part of the incident light intensity at the outer and inner surfaces of the cuvette windows and to light scattering inside the solution (cf. Fig. 2.2). Therefore, it is convenient to compare the transmitted light of the sample cuvette to that of a similar reference cuvette containing only the solvent, thereby eliminating the role of all factors except for the absorption by the solute. If we denote the intensities transmitted behind the sample cuvette and the reference cuvette by I_S and I_R, respectively, when they are both hit by the same light intensity I_0, the transparence T as related to pure absorption is defined as

$$T = \frac{I_S}{I_R} \tag{2.1}$$

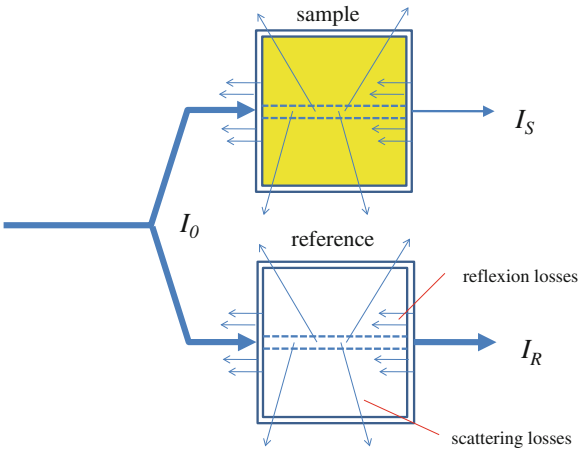

Fig. 2.2 Effects diminishing the transparency of a solution and separation of the absorption effect of the solute by comparing sample and reference

According to Lambert's law, T decreases exponentially with the optical path length d of the light (cf. Fig. 2.3):

$$T = 10^{-k \cdot d} \tag{2.2}$$

The attenuation factor k is specific for the given solute, its concentration and the wavelength of the light. According to Beer's law it is proportional to the concentration c of the absorbing compound:

$$k = \varepsilon(\lambda) \cdot c \tag{2.3}$$

Here $\varepsilon(\lambda)$ is the molar decadic absorption coefficient. Although the penetration of light into an absorbing medium does not come to an end sharply, as shown in Fig. 2.3, the typical "penetration depth" is conventionally characterized by a finite length, given by

$$d_p \equiv \frac{1}{k \cdot \ln 10} \tag{2.4}$$

After a path length d_p, the light intensity has dropped to about 37 % of its initial value.

Equation (2.3) is the basis for quantitative analytical determinations by photometry. Here it is customary to introduce the absorbance A as a new quantity which is directly proportional to the concentration c:

$$A \equiv k \cdot d = \varepsilon \cdot c \cdot d \tag{2.5}$$

Introducing this expression into Eq. (2.2) we arrive at Lambert–Beer's law

$$T = 10^{-A} \tag{2.6}$$

$$A = -\lg T \tag{2.7}$$

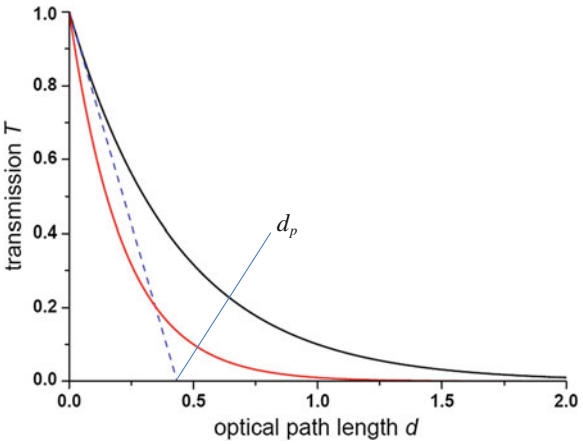

Fig. 2.3 Lambert's law for transmission T as a function of optical path length d for two attenuation factors $k = 1$ (*black curve*) and $k = 2$ (*red curve*). The *dashed line* indicates the definition of the "penetration depth" d_p

Customary spectrophotometers automatically record the wavelength dependence of the absorbance. Such records are called absorption spectra. Other than transmission spectra, they exhibit strict proportionality to the concentration of the sample at any wavelength (cf. Fig. 2.4). However, one should take care of spectral changes that may occur upon associations of molecules at higher concentrations.

2.1.3 Theoretical Basis of Absorption Spectra

The simplest appearance of absorption spectra is found for isolated atoms in the gas phase. These spectra exhibit isolated sharp absorption lines, i.e., very narrow ranges of wavelength where light absorption does occur. As was first shown by Bohr, these lines (more easily detected as emitted light after excitation of the atoms) reflect the pattern of energy quantization in the atoms. A key to his theory was Einstein's suggestion that the energy of light is quantized, whereby the energy E_{ph} of the light quanta (photons) is determined by the frequency v of the light:

$$E_{ph} = hv \tag{2.8}$$

Since, for a wave with frequency v and wavelength λ the following equation holds

$$v \cdot \lambda = c \tag{2.9}$$

where c is the speed of light, the photon energy can be also expressed by the wavelength

$$E_{ph} = \frac{h \cdot c}{\lambda} \tag{2.10}$$

According to Bohr's postulate, light can be only absorbed if the photon energy exactly matches the energy difference between two possible energy states n and m of the atom.

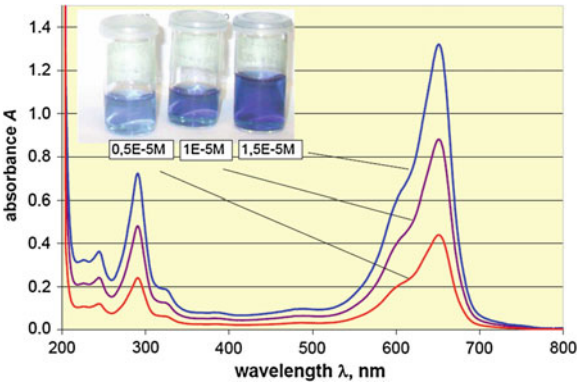

Fig. 2.4 Absorption spectra of methylene *blue* in methanol at three different concentrations. According to which the absorbance can be calculated from the measured transmission T by

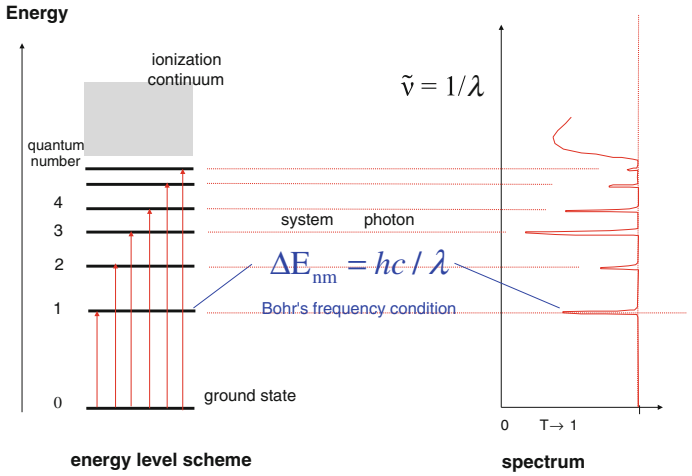

Fig. 2.5 Relation between absorption spectrum (*right*) and energy level scheme (*left*) in isolated atoms. The absorption spectrum, when plotted on a frequency scale, represents an image of the energy level scheme of the atom

$$\Delta E_{nm} = \frac{hc}{\lambda} \tag{2.11}$$

In case of an absorption spectrum, it is usually the energy spacing between the ground state, the *normal* state of the atom, and any of its higher (i.e., *excited*) states. These ideas are illustrated in Fig. 2.5.

In case of molecular compounds in condensed media, the typical appearance of the absorption spectrum is as shown for the example of methylene blue in Fig. 2.4. It is characterized by an almost continuous absorption across the full wavelength range, however structured by broad absorption peaks and broad minima. The absorption peaks exhibit spectral widths of some 50–100 nm and they differ in their absolute heights (intensities). The spectral regions of the peaks are termed absorption bands. In the following we will clarify three questions:

1. What determines the positions of the bands?
2. What determines the widths of the bands?
3. What determines the intensities of the bands?

The explanations are illustrated by Fig. 2.6. Here, a schematic absorption spectrum of chlorophyll a is plotted over a vertical axis. We realize that, with reference to Eq. (2.10), the scales of photon energy and wavelength run in opposite directions. As in the atomic case, in the molecular case, too, the energy scale of the absorbed light has to be seen against the energy scale of the molecular energy levels.

A molecular energy level scheme comprises much more levels than an atomic one, where energy can be only deposited in the form of electronic excitations. In molecules, the atoms can vibrate against each other. They can do so in N-6 modes

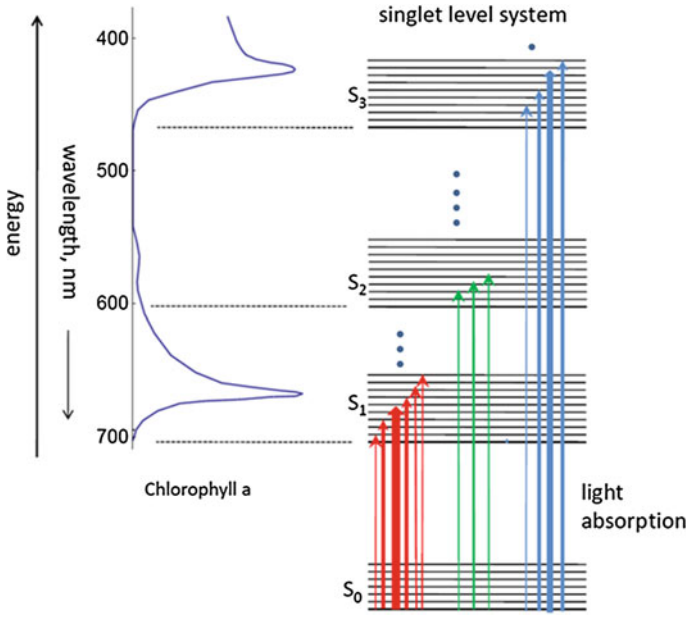

Fig. 2.6 Molecular energy level scheme and its relation to the molecular absorption spectrum. For details cf. text. Adapted with permission from Ref. [12], Schmidt W, Optische Spektroskopie, p. 58, Copyright © 2000 Wiley–VCH Verlag GmbH & Co KGaA

(*N*-5 in linear molecules). The vibrational energy of each of these modes is quantized in multiples of $h\nu_{vib}$, where ν_{vib} is the vibrational frequency of the mode. Thus, their energy level schemes represent uniformly spaced ladders with step widths much smaller than typical electronic excitation energies, but extending (as indicated by the dots in Fig. 2.6) up to typical bond breakage energies which are normally larger than the spacing between the electronic levels. In Fig. 2.6, the vibrational level structure is represented in a very schematic way, displaying just the vibrational progression of one representative mode. In reality *N*-6 (or *N*-5 if it is a linear molecule) such vibration energy ladders have to be superimposed. Since different vibrational modes can be excited to various degrees at the same time, the number of possible combinations of vibrational states increases drastically with increasing total vibrational energy.

Apart from electronic excitation and vibration of the nuclei, a molecule can also rotate, which adds another, still finer level substructure to the one depicted in Fig. 2.6. In solution, these rotational levels are broadened, because free rotations are hindered. Therefore, the total level scheme of a molecule in solution essentially corresponds to a continuum which accounts for the apparent continuous nature of the absorption spectrum. Nevertheless, the band structure of molecular absorption spectra shows, that on absorption of a photon, the transitions to any of the electronic-vibrational-rotational (*rovibronic*) states are not equally probable. In the first place, it is still the interaction of the electromagnetic light wave with the

electrons that is responsible for photon absorption. The excitation of an electron occurs on a much shorter time scale than the period of a molecular vibration, such that, on the time scale of a vibration, the electronic excitation is practically instantaneous. Since the valence electrons excitable by light are responsible for the chemical bonds and for the forces on the atoms, when they vibrate out of their equilibrium positions, a rearrangement of the electron distribution on excitation may result in a change of forces between the atoms and thereby, after excitation, the molecule will start to vibrate stronger or weaker than before it was excited. The particular values of the shifts of vibrational potential curves between electronic ground and excited states will determine which electronic-vibrational (*vibronic*) level combination will have the highest probability of excitation. In a qualitative way, this relation is expressed in the Franck–Condon principle, in a quantitative way the intensity distribution over an absorption band is determined by the Franck–Condon factors of the vibrational levels that are connected by the transition. In general, the position of a band maximum, i.e., the vibronic transition of highest probability, is not too far from the pure electronic transition. Therefore, the pattern of the band maxima positions is rather close to the purely electronic energy level scheme of a molecule. The widths of the bands are determined by the extent to which vibrations are excited together with the electron, and are therefore governed by the Franck–Condon principle.

The electronic excitation energies can be qualitatively estimated from the molecular orbital picture of the electronic structure. In molecules it is customary to classify the orbitals according to their nodal properties with respect to the chemical bonds (cf. Fig. 2.7). If an orbital wave function does not change its sign when orbiting around a chemical bond, it is classified as a σ-orbital. If there are two sign changes on a full circle around a bond, it is classified as a π-orbital. If there is no node along the chemical bond, the orbital is bonding, i.e., it causes attraction of the adjacent atoms. Orbitals with a node along the bond are antibonding, i.e., they cause repulsion between the adjacent atoms if populated by an electron. Antibonding orbitals are denoted by an asterisk in combination with the Greek symbol.

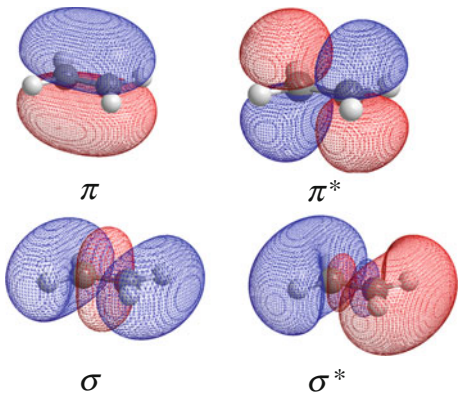

Fig. 2.7 Representation of σ, σ^*, π, and π^* molecular orbitals in ethylene

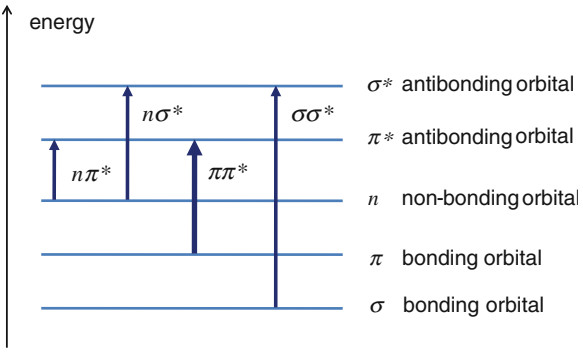

Fig. 2.8 Schematic overview of characteristic types and energy ordering of electronic transitions in molecules

In organic compounds containing atoms other than hydrogen and carbon, so-called hetero atoms such as nitrogen and oxygen, some of the electron pairs of the heteroatom do not participate in bonding or antibonding. These are called *n*-electrons (nonbonding electrons).

Roughly, the energetic order of the various types of molecular orbitals is: σ, π, n, π^*, σ^*. Electronic transitions between these orbitals are assigned the labels of the orbitals involved. Hence, we may distinguish $n\pi^*$, $n\sigma^*$, $\pi\pi^*$, and $\sigma\sigma^*$ transitions which are typically ordered in energy as shown in Fig. 2.8. The bands in the visible are usually of $n\pi^*$ or $\pi\pi^*$ nature.

Finally, we are left with the third of the questions posed above, regarding the intensity of the electronic absorption bands. This intensity can be interpreted as the probability per time unit of a molecule to undergo a certain transition in an electromagnetic field of a given wavelength and strength, or else as the probability of absorption of a photon of a given energy on passing a certain number of uniformly distributed molecules. This process requires electric interaction between the electrons and the light field. Classically, it can be described in analogy to the absorption of energy by an oscillating dipole antenna in a radio wave field. We should note, however, that the energy eigenstates of the molecule are stationary, i.e., there is no oscillation of the electrons that could represent the dipole antenna. Such a situation, i.e., real oscillation of charge, occurs only when different energy eigenstates are coherently superimposed or mixed. Then the electron cloud oscillates with a frequency given by Bohr's condition, Eq. (2.11). The rate at which this oscillator takes up energy from the radiation field is proportional to the square of the electric dipole moment of the oscillating charge. The charge distribution of the oscillator can be obtained by multiplying the wavefunctions of the two states involved in the transition. We will demonstrate this procedure for the transition between the highest occupied molecular orbital (HOMO) and the lowest unoccupied molecular orbital (LUMO) in naphthalene. Since these orbitals are π-orbitals, we are dealing with a $\pi\pi^*$ transition. In Fig. 2.9, the representations of the orbitals and of the transition charge density distribution are shown. The charge distribution can be assigned to four partial dipoles, two weak ones pointing downward, two strong ones pointing upward. Thus, there is a resultant transition

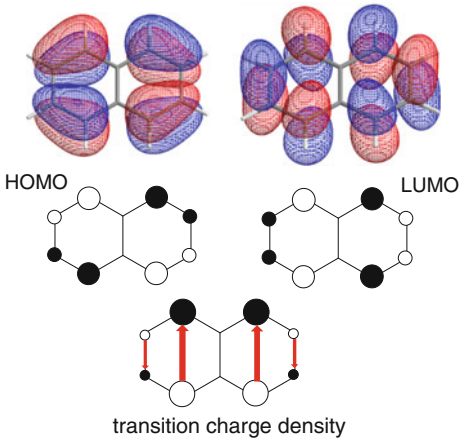

Fig. 2.9 HOMO and LUMO of naphthalene. *Upper row*: isocontour plot from an extended Hückel calculation. Middle row: Hückel MO coefficient representation, *Lower row*: HOMO → LUMO transition charge density with partial dipoles. *Black* and *white circles* represent positive and negative values, respectively, of molecular orbitals and the charge density

dipole moment along the short axis of the naphthalene molecule, meaning that this transition can absorb energy from a radiation field where the electrical vector oscillates (is polarized) parallel to the direction of the short axis.

The HOMO–LUMO transition in naphthalene gives rise to a moderately strong absorption band with a maximum absorption coefficient of about 6,000 M^{-1} cm^{-1}. It corresponds to the second band in the spectrum shown in Fig. 2.10. Note that a log-scale is used for the absorption coefficient in order to accommodate bands of very different intensity in one diagram. It is also worth of note that, in general, excited electronic states cannot be precisely described by a single electron configuration as we have assumed for the HOMO → LUMO excitation in naphthalene, where it is rather well justified. In general, one has to mix different electron configurations to arrive at a realistic description of a specific excited state. For example, in naphthalene the first and third excited states are approximately obtained from combining two configurations, one involving excitation of an electron from the HOMO to the LUMO + 1 orbital and the other from the HOMO-1 orbital to the LUMO orbital. Their combinations result in a lowest excited state with a very small transition dipole moment (band ① in Fig. 2.10) and in the third excited state with a very large transition dipole moment (band ③ in Fig. 2.10) in the transition from the ground state to these states. For different types of transitions, the absorption coefficients can vary over a very wide range. An overview of typical cases and orders of magnitude is presented in Table 2.1.

2.1.4 Photophysical Processes in the Excited State

The general "map" for the processes taking place after electronic excitation of molecules is the so-called Jablonski scheme shown in Fig. 2.11 [4]. It shows two energy ladders, termed the singlet and the triplet system. Singlet and triplet refers to the spin multiplicity of an electronic state. In a singlet state, the spins of all

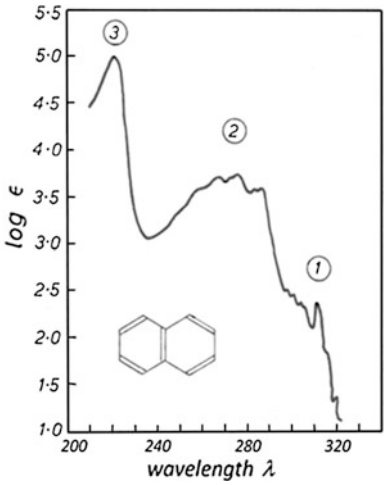

Fig. 2.10 UV absorption spectrum of naphthalene in ethanol. Reprinted from Ref [13], Murrell JN (1963) The theory of the electronic spectra of organic molecules. Methuen & Co, London, reproduced with permission by J. N. Murrell

Table 2.1 Typical ε_{max}-values of light-absorbing compounds

Category	ε_{max}	Class of compounds and orbitals involved
Strong absorption	5,000–100,000 M^{-1} cm^{-1}	Organic dyes, acid/base indicator dyes, π-orbitals
Medium strong absorption	500–5000 M^{-1} cm^{-1}	Complexes of subgroup elements with π-electron ligands (e.g., MnO_4^-, $Fe(SCN)_3$) charge transfer transitions between metal *d*-orbitals and ligand π-orbitals (LMCT, MLCT-transitions)
Weak absorption	<100 $M^{-1}cm^{-1}$	E.g. aquo-, ammin-, chloro- fluoro- complexes of subgroup elements d-electrons of the metal ions
Very weak absorption	<1 $M^{-1}cm^{-1}$	Ions of rare earths f-orbitals of the metal ions

electrons are paired and the total spin is zero. For normal molecules with an even number of electrons, this is generally the case for the ground state which is therefore given the term symbol S_0 (for the exception of molecular oxygen cf. below). In a triplet state, the spin angular momentum of two unpaired electrons adds up to a spin quantum number of 1. Since three different spatial orientations of such a spin can be distinguished, the multiplicity of the state is 3, hence the term triplet state. On excitation, at least two electrons will reside in singly occupied molecular orbitals. Hence the Pauli principle does no longer restrict their mutual spin alignment and singlet states as well as triplet states are possible. For states that can be described by a single electron configuration, the triplet state is usually at lower energy than the singlet state because in triplet states the unpaired electrons still do avoid close encounters due to the Pauli principle, and therefore their average repulsion energy is less than for the corresponding singlet configuration.

Radiationless transitions. Let us follow the fate of a molecule after its excitation to a higher vibronic (i.e., electronically and vibrationally excited) state.

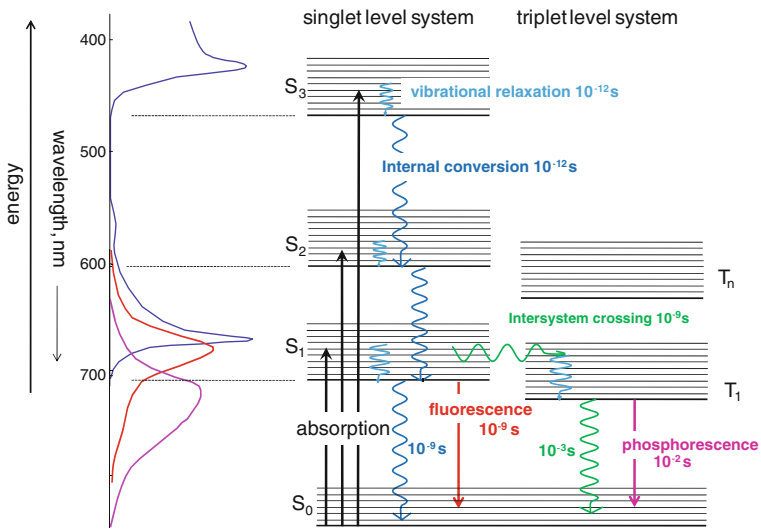

Fig. 2.11 Jablonski scheme representing the typical photophysical processes in molecules. For details cf. text. The time constants given are to be understood as typical orders of magnitude. Deviations from these typical values by one or two orders of magnitude may be found in specific systems. Adapted with permission from Ref. [12] Schmidt W, Optische Spektroskopie, p. 58, Copyright © 2000 Wiley–VCH Verlag GmbH & Co KGaA

Vibrational excitation means that the molecule is in a "hot" state. In a condensed medium, there are many collisions between the molecule and its surroundings, and the excess vibrational energy is easily transferred to the "cold" molecules of the medium. Thus, within typically an order of magnitude of 10^{-12} s, the molecule has undergone a *vibrational relaxation* to the more or less vibrationless excited electronic state. Further relaxation requires the intramolecular transformation of electronic energy into vibrational energy which is termed *internal conversion*. Since the steps of the electronic energy ladder are usually much larger than the vibrational energy quanta, such a transformation goes along with a strong change in the motional state of the nuclei and it is the harder to realize the larger the electronic energy gap (so-called energy gap law). Typical times for internal conversion steps between the higher excited states are on the order of 10^{-12} s. Since the energy gap between S_1 and S_0 is usually larger than between the higher states, the $S_1 \rightarrow S_0$ internal conversion is much slower, typically on the order of 10^{-9} s. A famous exception to this behavior is the case of azulene, where the $S_2 \rightarrow S_1$ internal conversion is much slower than the $S_1 \rightarrow S_0$ one, which however also reflects the rule of the energy gap law, because the $S_2 - S_1$ energy gap is exceptionally high in that case.

Intersystem Crossing. Changing an electronic state from singlet to triplet requires a spin flip of one of the unpaired electrons. Such processes can be only achieved by the action of an effective magnetic field. The magnetic component of

the light field is too weak to compete with the effects of the electric field component while it induces an electronic transition between different orbitals. However, there is an intramolecular perturbation, spin–orbit coupling, which can cause spin flips during radiationless and radiative transitions.

Spin–orbit coupling is a relativistic effect that may be visualized as the action of an effective magnetic field seen by the electrons while orbiting around the charged nuclei. Seen from the electron, the relative motion of the nucleus in an atom corresponds to a ring current that produces a magnetic field along which the electron spin tends to align. The effect increases linearly with the orbital momentum of the electron, but much more strongly (to the fourth power) with the nuclear charge. In nonlinear organic molecules, the molecular orbitals have little directed orbital momentum. Thus, spin–orbit coupling effects in such molecules are usually weak and hence there is little mixing between singlet and triplet states. However, spin–orbit coupling effects can be enhanced by the presence of heavy atoms (i.e., with nuclei of high electric charge) and/or during transitions between orbitals that involve a rotation of a p-orbital at some hetero atomic center, such as occurring e.g., in transitions between $n\pi^*$ and $\pi\pi^*$ excited states. Therefore, radiationless (and radiative, c.f. below) intersystem crossing processes are particularly effective between singlet and triplet states differing in their electronic orbital nature.

Apart from the strength of spin–orbit coupling between two electronic states, the electronic energy gap between them is the second important factor for the rate of a radiationless transition between a singlet and a triplet state or vice versa. The energy gap law holds in this case, too, just as for internal conversion processes between states of the same multiplicity. Therefore, the radiationless transition from T_1 to S_0 is much slower than from excited singlets to the triplet system. Typical orders of magnitude are 10^{-9} s for the latter and 10^{-2} s for the former. However, such numbers should be taken with care, because deviations by one or more orders of magnitude are possible, depending on the specific case.

Photoluminescence. When looking at dye solutions, one often can observe some extra "glow" in the sample, adding to the spectrally filtered transmitted light (cf. the photo of methylene blue bottles in Fig. 2.4). This phenomenon is due to a spontaneous, undirected emission of light and its spectral characteristics are specific for the emitting molecules, but rather independent of the wavelength of the light absorbed. Spectrally, this photoluminescence appears in a band positioned on the long wavelength side of the first absorption band and with a band shape resembling a mirror image of that absorption band. (cf. Fig. 2.11). If excited by a very short light pulse of less than a nanosecond, it is possible to observe the decay of the photoluminescence in time and to distinguish two components of very different life time: a short one, *fluorescence*, with a life time characteristic of the S_1 state and a long-lived one, *phosphorescence*, with a life time characteristic of the T_1 state. While the fluorescence intensity may come close to the intensity of the absorbed light (i.e., may reach a quantum yield of 1), at room temperature, the phosphorescence is usually very weak because the emission is spin-forbidden and its rate is much smaller than the rate of radiationless deactivation of T_1. Thus, the

quantum yield of phosphorescence is small under such conditions. At low temperatures, in rigid matrices, however, the radiationless transitions may be slowed down to an extent that the phosphorescence quantum yield can become appreciable, too.

The independence of photoluminescence spectra of the wavelength of absorption, known as Kasha's rule, is a consequence of the energy gap law making electronic energy relaxation by internal conversion fast until the S_1 or T_1 state is reached. Only here, further radiationless deactivation is slow enough for an emission process to compete. In principle, emission can also occur from a higher excited state, but the quantum yields of such processes are very low because of the dominance of radiationless deactivation processes. The exception of azulene has been mentioned above. The mirror image rule for the relation between first absorption band and photoluminescence band is rationalized by the Franck–Condon principle. It predicts similar intensities for transitions between vibronic states with the same combination of vibrational quantum numbers, irrespective of whether the higher vibrational quantum number is associated with the ground state or the excited state (Fig. 2.12).

Electronic energy transfer. For many situations in nature and technology, it is important that electronically excited states cannot only be produced by direct absorption of light, but also by accepting the electronic energy through a radiationless pathway from some other electronically excited species that has absorbed the light in the first place. Examples of such processes can be found in photosynthesis and in bioanalytical applications (vide infra). The production of molecular singlet oxygen, a reactive key species in photodynamic therapy, is another case of particular interest for this book. Like the probability of the absorption of photons, the rates of electronic energy transfer processes are subject to specific rules. In the latter case, these are mainly concerned with the conservation of spin and the

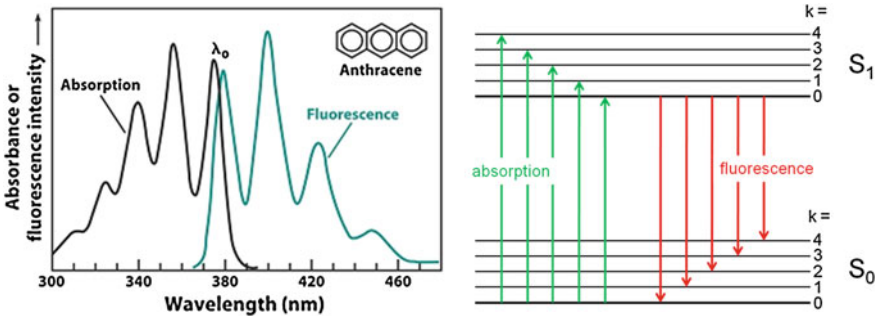

Fig. 2.12 Mirror-image relationship between absorption and emission exemplified for the case of fluorescence of anthracene. *Left*: fluorescence and absorption spectrum (the latter recorded by the intensity change of fluorescence at a fixed wavelength as the excitation wavelength is scanned). Adapted with permission from ref [14]., Byron CM, Werner TC, J Chem Educ 1991, 68:433–436. Copyright © 1991 American Chemical Society. *Right*: correspondence scheme for vibronic transitions. For details cf. text

distance dependence of the energy transfer rate between the energy donor and the energy acceptor. It is in compliance with the spin conservation criterion that a donor in an excited singlet can transfer its energy to an acceptor in a singlet ground state, when the donor undergoes a transition to its singlet ground state and the acceptor ends up in an excited singlet state, usually in the S_1 state. This type of energy transfer is termed singlet–singlet energy transfer, or—according to its most prominent mechanism—Förster *resonance energy transfer*. In practical applications it also goes by the name of *fluorescence resonance energy transfer*. The acronym FRET allows for both readings. In case of triplet excited donors, the spin conservation principle allows only for the creation of triplet excited acceptor molecules, if their ground state is singlet. However, in the case of acceptors with a triplet ground state, spin-allowed energy transfer from triplet excited donors leads to excited singlet states. The case of molecular oxygen (cf. below) is a prominent example. Let us consider the FRET case first (cf. Fig. 2.13). As described above, shortly after its photoexcitation, a donor is usually in its vibrationless first excited singlet state, which has a typical lifetime of about 1 ns. A close-by acceptor molecule can directly "sense" the electric field of the transition dipole related to the electronic excitation of the donor and it can take up its energy if there is a resonance, i.e., an exact energy matching with an electronic transition in the acceptor. This process does not require the spontaneous emission of a photon by the donor but takes place in a radiationless fashion. The mechanism of the energy transfer is based on the dipole–dipole interaction between the transition dipole moments of donor and acceptor. The energy of the interaction between the two transition dipoles is proportional to the strength of the transition dipoles and to the inverse of the third power of the distance R between donor and acceptor. Since the rate of the energy transfer process is proportional to the square of the interaction energy, it depends on

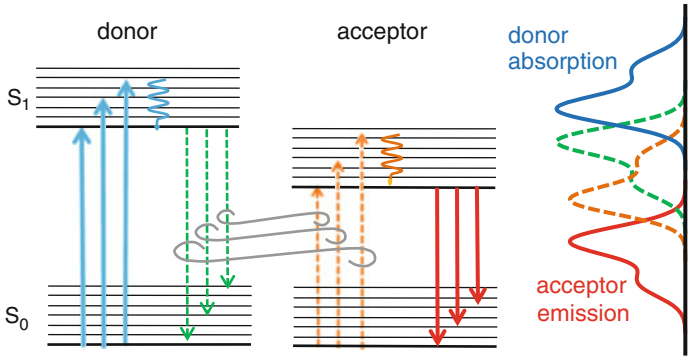

Fig. 2.13 Principle of the FRET process. The concerted transitions of donor and acceptor require energy matching of fluorescence of the donor (*dashed green arrows* and spectrum) and absorption of the acceptor (*dashed orange arrows* and spectrum). However, they occur without emission of the donor. After the energy transfer to the acceptor, its specific fluorescence spectrum can be observed (*red arrows*, spectrum)

the distance R as the inverse of the sixth power of R. This leads to the famous Förster relation for the rate constant k_{FRET} of this type of energy transfer:

$$k_{\mathrm{FRET}} = k_0 \left(\frac{R_0}{R}\right)^6 \tag{2.12}$$

Here k_0 stands for the rate constant of spontaneous deactivation of the excited donor and R_0 is the so-called Förster radius. At this separation of donor and acceptor, the rate constant of energy transfer and spontaneous decay of the excited donor are equal, i.e., under such conditions the overall decay rate of the donor is two times as fast as in the absence of an acceptor and the efficiency of energy transfer amounts to 50 %. The value of the Förster radius R_0 is determined by the strength of the two interacting transition dipoles. As Förster has shown, the resonance condition and the role of the strengths of the two transition dipoles can be exactly described by the overlap of the fluorescence spectrum of the donor and the absorption spectrum of the acceptor. Nevertheless, the process does not involve spontaneous emission of a photon by the donor and its reabsorption by the acceptor. Donor and acceptor pairs with good interaction are characterized by high values of R_0 which in favorable cases may reach values as high as 50–80 Å. In bioanalytical applications, FRET experiments, even with single molecule resolution, have become a convenient tool to probe distances and conformational changes within complexes of biomacromolecules.

If suitable donor and acceptor molecules are fixed on conformationally mobile parts of a biomacromolecular complex their separation will undergo a dynamic change. Preferentially, the range of distances should comprise the Förster radius R_0. In such a case, the efficiency of energy transfer will undergo appreciable changes which can be read from the ratio of fluorescence intensities of donor and acceptor. Figure 2.14 shows a prominent recent example [15], where single molecule emission is used to probe the dynamics of the donor–acceptor distance and thereby the systematic motion of the rotating part of F_0F_1-ATPase of *Escherichia coli*. Using this technique, it can be demonstrated how the sense of the rotation changes with the environmental conditions under which ATP is synthesized or hydrolyzed, respectively.

Triplet–triplet energy transfer. Since excited triplet states live much longer than excited singlets, the chance that they can transfer energy before they decay is higher, or can be effected with the same efficiency at lower concentrations of the acceptor species. As with singlet–singlet energy transfer, there is also conservation of the overall spin in triplet–triplet energy transfer processes. Whereas, however, there is spin conservation in each of the partners of a singlet–singlet energy transfer, there is spin conversion from triplet to singlet in the donor and singlet to triplet in the acceptor. Therefore, this process is not induced by the coupling of two transition dipole moments, which are very weak for spin-forbidden transitions, and it does not have a long-range character as in the Förster mechanism. Efficient triplet–triplet energy transfer is made possible by the synchronous exchange of two electrons related to the two singly occupied orbitals in each of the two species

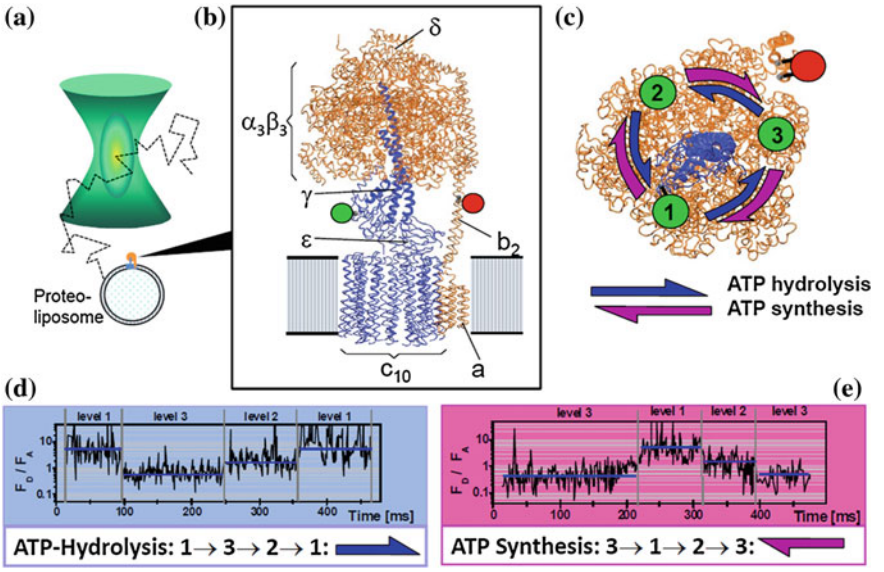

Fig. 2.14 Application of single molecule FRET to detect the three stages of ATPase operation in ATP synthesis and hydrolysis [15]. **a** Fluorescence from a fluorescence labeled ATPase molecule on a proteoliposome is detected while the latter diffuses through the focus of a laser beam. **b** Side view of model of F_0F_1-ATPase from *E. coli.* The FRET donor (*green circle*) is bound to the γ subunit, the FRET acceptor (*red circle*) to the b subunits. 'Rotor' subunits are *blue*, 'stator' subunits are *orange*. **c** Cross-section at the fluorophore level. During enzyme action the FRET donor on the rotor part adopts the sequence of positions 1, 2, and 3, differing in distance to the static FRET acceptor, such that energy transfer is most efficient in position 3 and least efficient in position 1. **d** Time-dependent record of acceptor/donor fluorescence ratio under ATP hydrolysis conditions. **e** Under ATP synthesis conditions. Note that the time sequence of positions 1–3 is reversed between situations **d** and **e**. Adapted from Nature Structural and Molecular Biology 11:135–141, Copyright © 2004 Macmillan Publishers Ltd. Adaptation by courtesy of Prof. C.A.M Seidel

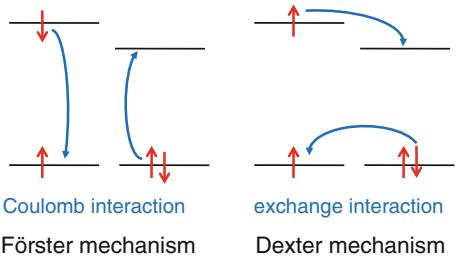

Fig. 2.15 Illustration of concerted, spin-conserving two-electron motion in the Förster and the Dexter mechanism of electronic energy transfer in singlet–singlet and triplet–triplet energy transfer, respectively

involved in the process. This principle is depicted in Fig. 2.15. The so-called exchange mechanism was first suggested by Dexter. It requires some spatial overlap of the electronic wavefunctions of the two species which can be only achieved if the two molecules get into close contact.

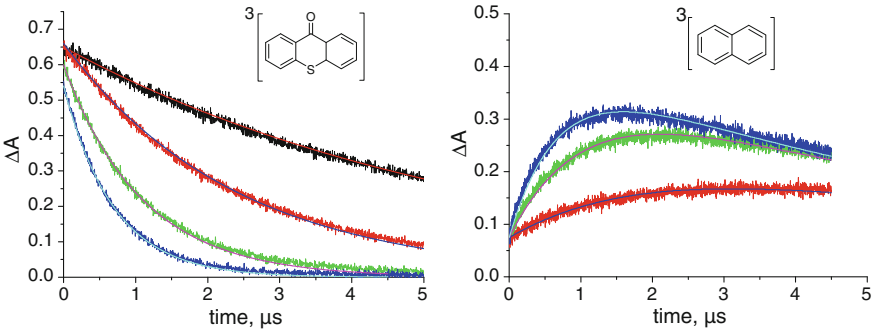

Fig. 2.16 Experimental example of triplet–triplet energy transfer between thioxanthone triplet (donor) and naphthalene (acceptor). Transient absorption signals are shown for two wavelengths, where characteristic absorptions of the two triplets are found. *Left*: transient absorption of thioxanthone triplet for (from *above*) concentrations 0, 0.1, 0.3, 0.5 mM of naphthalene. *Right*: transient absorption of naphthalene triplet for (from *below*) concentrations of 0.1, 0.3, and 0.5 mM of naphthalene

In Fig. 2.16, an example of the observation of triplet–triplet energy transfer is shown. Here, thioxanthone is the triplet energy donor and naphthalene the acceptor. Since, at room temperature, phosphorescence is usually too weak, an observation by transient absorption is the standard method of detection for triplets at ambient temperatures. As with singlet–singlet energy transfer, a matching of energies of donor and acceptor triplets is a condition for an efficient process in the case of triplet–triplet energy transfer, too. As in the former case, electronic energy transfer also comprises the excitation of vibrations (cf. Fig. 2.13) the probability of which is controlled by the Franck–Condon principle (cf. the special example of singlet oxygen formation below). Since the donor usually ends up in some vibrationally excited ground state and the acceptor in a vibrational excited triplet state, the best conditions for energy matching are given if the purely electronic energy of the donor is higher than that of the acceptor, i.e., $E_T(D) > E_T(A)$.

Singlet oxygen formation by electronic energy transfer [5]. In photodynamic therapy, singlet excited molecular oxygen plays a central role. Figure 2.17 shows the electron configurations related to the lowest electronic states of molecular oxygen. They differ in the populations of the lowest π^* orbitals. These orbitals represent the antibonding combinations of the atomic p-orbitals having their axis perpendicular to the molecular axis. In Fig. 2.17, the representations of two real-valued orbitals termed LUMO a and LUMO b are shown. The orbitals LUMO a and LUMO b represent wave functions with an orbital angular momentum of quantum number 1. But the sense of the electron rotation around the molecular axis, i.e., whether it is a right-hand or left-hand turn, is not defined for these orbitals. Instead, they represent situations where right and left sense rotation are equally mixed. The π orbitals $\pi_{\pm 1}^*$ are obtained from them as symmetric and antisymmetric linear combinations but with the imaginary number $\pm i$ as a phase factor. The complex orbitals π_{+1}^* and π_{-1}^* represent states with sharply defined

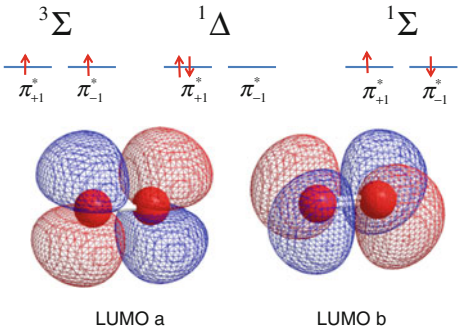

Fig. 2.17 Orbital configurations of the lowest electronic states of molecular oxygen. The states differ in the two-electron configuration of the degenerate two π^* orbitals. For details cf. text

right or left sense rotations, respectively. In an isolated O_2 molecule, these states are exactly degenerate for symmetry reasons.

In the lowest electronic state of O_2, i.e., in its ground state, each of the two π^* orbitals is singly occupied and the spins of the two unpaired electrons are parallel, according to Hund's rule. Hence the ground state of O_2 is a triplet state and therefore paramagnetic. Since the orbital angular momenta of π^*_{+1} and π^*_{-1} are equal, but opposite in sign, they cancel each other, so that the total orbital angular momentum is zero. This fact is expressed by the term symbol Σ. If both electrons share the same π^*orbital, their spins must be opposite, such that the total spin is zero. On the other hand, their orbital angular momenta add up to a quantum number of 2 for the total orbital angular momentum. These properties are denoted by the term symbol $^1\Delta$. Finally, if the two electrons are in different π^* orbitals, but with opposite spins we generate a singlet state with total orbital angular momentum quantum number 0, i.e., a $^1\Sigma$ state. One should note that the single configurations shown in Fig. 2.17 for $^1\Sigma$ and $^1\Delta$ do not give the full representation of the wave functions of the two states. The full wave functions include the complementary configurations, too, where the populations of the two π^* orbitals are just exchanged. The energies of the two lowest excited states of O_2 are 94 kJ/mol ($^1\Delta$) and 157 kJ/mol ($^1\Sigma$) above the $^3\Sigma$ ground state. The energy differences are due to the differences in electron–electron repulsion reflecting the different average distances between the two electrons for the different configurations.

Singlet-excited oxygen can be produced by energy transfer from donors in excited singlet or triplet states. In case of excited singlet state donors, spin conservation requires that these undergo a transition from the excited singlet to the lowest excited triplet state. For energy reasons, the singlet/triplet gap must be greater than about 90 kJ/mol in order to populate the lowest excited singlet of oxygen. Furthermore, a diffusive encounter between molecular oxygen and the donor has to occur within a few nanoseconds, due to the short lifetime of the excited donor singlet. These conditions are not easy to fulfill in an effective way. Therefore, excited triplets as energy donors are the usual method to generate singlet excited molecular oxygen.

In Fig. 2.18, a scheme for the population and depopulation of excited states of molecular oxygen is shown. On encounter of the triplet donor and the triplet ground state oxygen molecule, the total spin of the pair can be 0, 1, or 2,

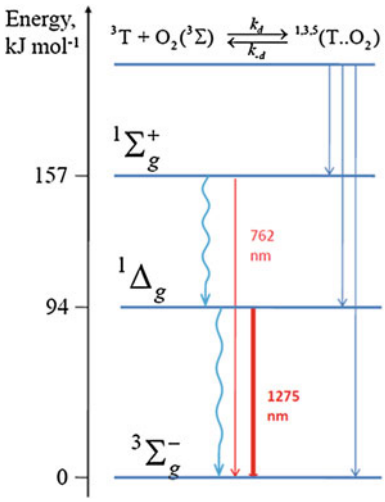

Fig. 2.18 Level scheme of lowest electronic states of molecular oxygen. Radiationless deactivation processes require interaction with surrounding molecules taking up the vibrational energy

corresponding to an overall singlet, triplet or quintet state, respectively. The statistical weights of these states are 1/9, 1/3, and 5/9, respectively. A deactivation of the encounter complex to a state comprising the singlet ground state of the donor and a singlet-excited oxygen species is only possible from the encounter complex with singlet multiplicity. However, there is rapid equilibrium between the encounter complexes in their different multiplicities [16], so that eventually all excited donor triplets may lead to the formation of singlet-excited oxygen, if the triplet lifetime is long enough. The ratio at which the two different singlet states of oxygen are formed is governed by the energy gap law (vide supra) [5]. In the encounter complex, the radiationless transition rate from the energy level of the excited donor to that of a specific excited state of oxygen is at a maximum for energy gaps between 0 and about 80 kJ/mol. For larger energy gaps, the rate quickly decreases. Thus, e.g., for 9-bromoanthracene, a triplet sensitizer with a triplet energy of 168 kJ/mol, the energy gap to both, the $^1\Sigma$ and the $^1\Delta$ state of oxygen is within the range of maximum rate and they are both populated with about 50 % probability [17]. On the other hand, for 2-acetonaphtone with a triplet energy of 248 kJ/mol, the energy gap to $^1\Sigma$ is 154 kJ/mol, i.e., in the region where the rate is strongly decreasing, but for the population of $^1\Delta$ with an energy gap of 91 kJ/mol the rate is still close to the maximum. This situation explains why, with this triplet energy donor, the $^1\Sigma$ and the $^1\Delta$ state of oxygen are formed at a ratio of 17:83 [17]. For most practical purposes, however, it is important to note that in condensed phases the radiationless deactivation of $O_2(^1\Sigma)$ to $O_2(^1\Delta)$ takes place on the nanosecond time scale and it is unimportant whether $O_2(^1\Delta)$ is formed directly in the encounter of triplet excited donor and ground state oxygen or through the $^1\Sigma$ state. It must be added, though, that in cases of donors with low oxidation potential, the encounter complexes of triplet donor and singlet ground state molecular oxygen may be deactivated through the intermediacy of a charge

transfer state, wherefrom the population efficiency of the two excited singlet states of oxygen is lower than in the previous mechanism [18].

In condensed media, the lifetimes of the two singlet-excited oxygen species differ by about six orders of magnitude [5]. They are determined by radiationless transfer of electronic energy to vibrational energy of the surrounding medium which can occur directly or, with higher rate, in the presence of charge transfer interaction. Particularly long lifetimes are observed in perhalogenated solvents such as CCl_4 with lifetimes of 130 ns for $O_2(^1\Sigma)$ and 31 ms for $O_2(^1\Delta)$. Particularly short lifetimes are observed in solvents with OH-vibrations, such as H_2O with a lifetime of 3.8 μs for $O_2(^1\Delta)$. That this behavior is due to the specific frequency of OH-vibrations, can be concluded from a much longer lifetime of 62 μs in D_2O.

In photodynamic therapy, the lifetime of singlet oxygen determines the average length d the excited oxygen molecule can diffuse away from the point where it was created. According to Einstein's square law

$$d^2 = 6D\tau \tag{2.13}$$

where D is the diffusion coefficient and τ the lifetime of the diffusing species. In living cells, the value of D for molecular oxygen is about 1.4×10^{-5} cm^2s^{-1} and the lifetime of $O_2(^1\Delta)$ 0.04 μs. Hence the diffusion length under such conditions amounts to about 20 nm [5].

2.2 Photochemistry and Photobiology

Photochemistry, in a modern sense, is the area dealing with chemical processes in electronically excited states [6–11]. Since such states are normally generated by the absorption of light, it is clear that only absorbed but not transmitted light can cause photoinduced chemical change. This principle was first stated as the Grotthus-Draper law. Because light is absorbed in units of photons, each molecule undergoing a photoreaction has to absorb a photon.[1] However, since electronically excited states may relax to the ground state by dissipating their excess energy either in radiative or radiationless processes, the probability that a molecule undergoes a chemical transformation after absorption of a photon is generally not unity. This probability is called the photochemical quantum yield of the photochemical process under consideration. The inverse of this quantity is the number of photons a molecule has to absorb on the average before it will undergo a photoreaction.

Just as normal thermal reactions, photoreactions, too, are characterized by certain changes of nuclear coordinates. The electronic energy as a function of the nuclear coordinates may be viewed as spanning a hypersurface of potential energy on which the nuclear system undergoes periodic vibrational motion and, in some

[1] This does not apply to radical chain reactions, where one absorbed photon may result in many product molecules.

cases, nonperiodic translocations, the latter representing chemical change and the path of lowest energy between the minima the reaction coordinate. Whereas, however, in a normal thermal reaction, the system never leaves the potential surface of the ground state, in a photoreaction, there is necessarily a cross-over from a higher potential surface to that of the ground state (*diabatic* change) where every reaction eventually must end. According to Förster [19], photoreactions may be classified according to the three cases depicted in Fig. 2.19. They are distinguished from each other by the way the system undergoes its transition to the ground state potential surface. In case (a), the chemical change is completely achieved in the excited state. Only after vibrational relaxation in the excited photoproduct the system undergoes a radiationless decay to the ground state. Such photoreactions are called *adiabatic*, because the potential energy hypersurfaces, representing the change of the total energy of the system under *adiabatically* slow motions of the nuclei, are also called *adiabatic* energy surfaces. Proton transfer reactions in the excited state represent the most prominent type of such adiabatic reactions. In case (b), a radiationless cross-over from the higher to the lower potential surface takes place before the configuration of a stable product is reached in the excited state. Such situations may occur, if potential minima on the excited energy hypersurface are situated between minima of the ground state hypersurface. Photochemical *cis/trans*-isomerizations provide examples of such reactions. Finally, in case (c), the chemical change occurs in the electronic ground state after radiationless deactivation of the excited state and with the aid of the vibrational excess energy, i.e., from a "hot" ground state, before this vibrational energy is dissipated to the environment.

Another important classification of photoreactions refers to their molecularity, i.e., whether they are intramolecular (monomolecular) of intermolecular (bimolecular). In the second case, the reaction partner of an excited molecule is usually a ground-state molecule. For such bimolecular reactions, the probability of a photoreaction, i.e., its photochemical quantum yield, depends on the concentration of the unexcited reaction partner.

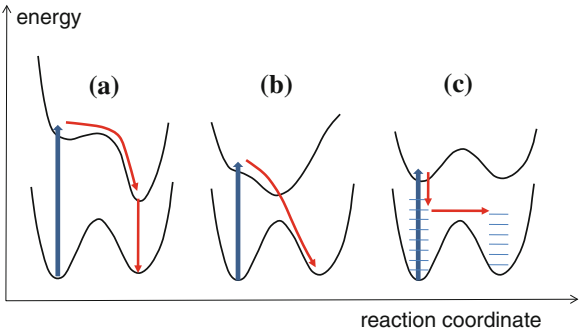

Fig. 2.19 Three cases of photochemical reactions according to Förster's classification [19]: **a** adiabatic photoreaction, **b** diabatic photoreaction, **c** hot ground state reaction. For details cf. text

Scheme 2.1 General reaction scheme of a bimolecular photoreaction competing with monomolecular deactivation

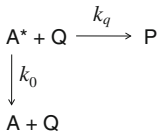

Accounting for the rates of the various processes in Scheme 2.1 we can derive the following expression for the photochemical quantum yield of product P from A*:

$$\Phi_P = \frac{k_q[Q]}{k_0 + k_q[Q]} \tag{2.14}$$

If there are no other deactivation channels, the quantum yield achieves a limiting value of 1 only for infinitely high concentration $[Q]$ of the ground state reaction partner. The concentration $[Q]_{1/2}$ at which half of the limiting quantum yield is attained, is determined by the rate constants k_q and k_0:

$$[Q]_{1/2} = \frac{k_0}{k_q} \tag{2.15}$$

After these general introductory remarks we will now regard some representative examples of elementary photochemical reactions.

2.2.1 Photoelectron Transfer Reactions

Photoexcitation caused by the absorption of light may be viewed as the separation of electron pairs, whereby one of the previously paired electrons is lifted up in energy into an empty orbital and a positive hole is left in the orbital where the electron came from. In this sense, the excitation is tantamount to an intramolecular charge separation. This is a rather formal view, however, since the involved orbitals normally penetrate each other strongly, such that the centers of gravity of the two orbitals may even coincide and no dipole moment results. Electron and hole can quickly recombine, a process denoted above as radiationless deactivation, and release the absorbed energy as heat to the environment. However, further spatial separation of (excited) electron and hole, as occurring by an electron transfer or hole transfer to a neighboring molecule and still further on, may occur with little loss of energy, but prevents rapid recombination of hole and electron. Thus, photo electron transfer reactions represent an ideal means of conserving light energy as chemical energy on longer time scales. This principle lies at the heart of natural processes such as photosynthesis and technical processes as used in photovoltaics (cf. Fig. 2.20).

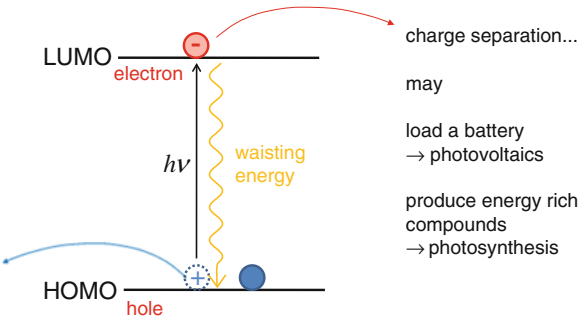

Fig. 2.20 Photoelectron transfer as a means of long-term storage of the photoexcitation energy

A general electron transfer reaction between an electron donor D and an electron acceptor *A* may be represented as[2]

$$A + D \rightarrow A^- + D^+ \tag{2.16}$$

The standard thermodynamic driving force of this reaction is given by the negative value of its standard Gibbs energy $\Delta G^{\ominus}_{et}$

$$\Delta G^{\ominus}_{et} = -F(E^{\ominus}(A^-/A) - E^{\ominus}(D/D^+)) \tag{2.17}$$

As expressed in this equation, $\Delta G^{\ominus}_{et}$ is determined by the difference of the standard electrode potentials for the reduction of *A*, $E^{\ominus}$ (A^-/A), and for the oxidation of *D*, $E^{\ominus}$ (D/D^+). The symbol *F* represents Faraday's constant. The more positive the value of $E^{\ominus}$ (A^-/A), the stronger *A* acts as an oxidant. Likewise, the more negative the value of $E^{\ominus}$ (D/D^+), the stronger *D* acts as a reductant. For organic molecules, these potentials are usually not strong enough to oxidize or reduce some other organic species. As shown in Fig. 2.21, the situation is, however, drastically changed, if *A* or *D* are electronically excited.

If the donor reacts from an excited state, the Gibbs free energy becomes more negative by the amount of the excitation energy of the donor:

$$\Delta G^{\ominus}_{et} = F \cdot (E^o(D/D^+) - E^o(A^-/A)) - E^*_D \tag{2.18}$$

Thus in an excited state a molecule is a stronger electron donor, i.e., a better reductant than in its ground state. Likewise, if the acceptor reacts from an excited state, the Gibbs free energy becomes more negative by the excitation energy of the acceptor:

$$\Delta G^{\ominus}_{et} = F \cdot (E^o(D/D^+) - E^o(A^-/A)) - E^*_A \tag{2.19}$$

Thus, in an excited state a molecule is also a stronger electron acceptor, i.e., a better oxidant than in its ground state.

[2] Here the charges should be considered as formal, because *A* and *D* themselves might be charged species, i. e. ions.

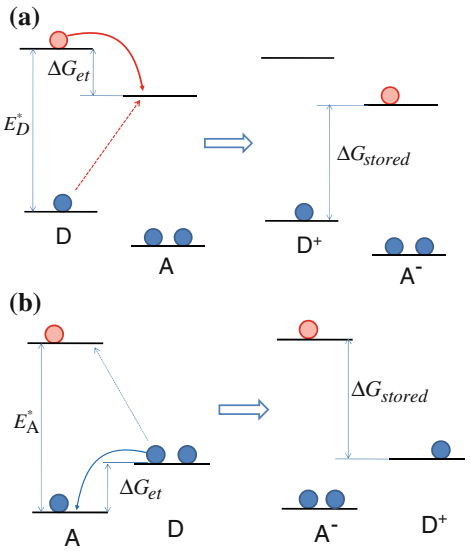

Fig. 2.21 Energetics of photoelectron transfer reactions. **a** Photoexcited donor. **b** Photoexcited acceptor. Photoexcitation makes a donor a stronger reductant and an acceptor a stronger oxidant. Excited state processes are marked with *solid curved arrows*. For comparison ground state processes are shown by *straight dashed arrows*

Due to these relations, photoinduced electron transfer reactions are quite frequent phenomena and, in many cases, these reactions are quite fast. This brings us to the question of how the rate of an electron transfer reaction and its thermodynamic driving force are related. It has been shown, both theoretically and experimentally that, other factors, such as the overlap of the electronic wavefunctions, determined by the separation between donor and acceptor, being equal, there is a strong correlation between the rate of electron transfer and the Gibbs free energy change of the process [4]. In Fig. 2.22, essential results are illustrated. In theoretical respect, the Marcus theory represented a great breakthrough [21–23]. Its main idea focuses on the change of the nuclear coordinates induced by the electron transfer and introduces the parameter λ, the so-called *reorganization energy*, corresponding to the change of electronic energy that would ensue if the system would adopt the nuclear configuration of the product but would remain in the initial electronic state present before the electron transfer. If $-\Delta G_{\mathrm{et}}$ is smaller than λ the electron transfer needs activation energy and the reaction gets faster the more negative ΔG_{et}. This is called the *normal* Marcus regime. If $-\Delta G_{\mathrm{et}}$ exceeds the value of λ the reaction is activationless and exergonic. The excess energy has to be converted to vibrational energy which is the same situation that led to the energy gap law of radiationless transitions, i.e., the rate decreases as ΔG_{et} tends to more and more negative values. This regime is called the *inverted* Marcus regime. In a brilliant series of experiments by Closs and coworkers this prediction of the Marcus theory was demonstrated to be correct [20].

The most important case of a photoinduced electron transfer reaction in nature is represented by the primary process of photosynthesis. The so-called photosynthetic reactions centers represent protein complexes containing a sophisticated

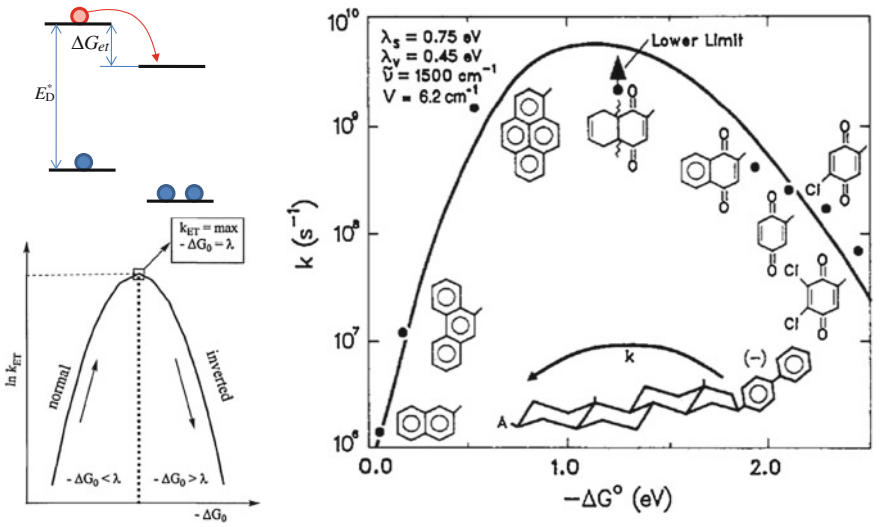

Fig. 2.22 *Left*: Schematic dependence of electron transfer rate constant on the free Gibbs energy (The ΔGet value determining the electron transfer rate in the encounter pair of donor and acceptor differs from the expressions given in Eqs. (2.18) and (2.19) by a term accounting for the different Coulomb energies of the donor/acceptor pair before and after the electron transfer. In polar environments, however, this term is usually small.) according to R. Marcus. In the "normal" region the electron transfer reaction needs to be activated, in the "inverted" region, the transformation of electronic excess energy into vibrational degrees of freedom is rate determining. The reorganization energy parameter λ determines the transition region. *Right*: Experimental verification of the Marcus prediction (Reprinted with permission from ref [20]., Miller JR, Calcaterra LT, Closs GL J. Am. Chem. Soc. 106:3047–3049. Copyright © 1984, American Chemical Society). The rate constant of electron transfer between the biphenyl anion rigidly connected to various electron acceptors is log-plotted versus the negative GIBBS free energy of the reactions. It should be noted that the symmetrical classical Marcus parabola is distorted with a gentler slope in the inverted Marcus region, if the quantum nature of nuclear vibrations is taken into account

arrangement of prosthetic groups controlling the primary electron transfer processes. Today, the structure of such reaction centers in photosynthetic bacteria as well as in plants is known to a high atomic resolution [25]. Figure 2.23 shows the active molecules and processes involved in a bacterial reaction center.

After excitation of the special pair, occurring mainly through singlet–singlet energy transfer from accessory antenna pigments, a photoelectron transfer to the first electron acceptor, a close-by bacteriochlorophyll molecule occurs within about 3 ps which is followed by an even faster hop-on process of the transferred electron to a pheophytin molecule. From here, the electron is transferred to an ubiquinone molecule, a process occurring in about 200 ps. Finally, with the intermediacy of a ferredoxin molecule, the ubiquinone in the second branch accepts the photoelectron, a process occurring on the time scale of about 10 μs. In purple bacteria, the electron returns from the final quinone acceptor to the oxidized special pair within about 1 s, thus completing an electron transfer cycle. The

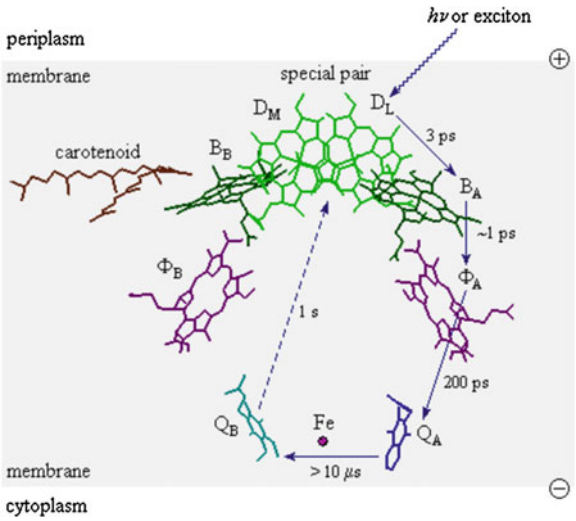

Fig. 2.23 Structure and primary photoelectron transfer pathways in bacterial reaction centers. Like in plants, these reaction centers consist of two almost symmetric branches comprising two bacteriochlorophyll molecules D_M and D_L, interacting directly with each other and representing the "special pair" D, two bacteriochlorophylls B_A and B_B, two bacteriopheophytins Φ_A and Φ_B and two quinones Q_A and Q_B. Only the *right*-hand side branch is active in the electron transfer process. Reprinted from http://metallo.scripps.edu/promise/PRCPB.html (cf. Ref. [24]) with permission by K. N. Degtyarenko

energetic benefit of the bacteria results from a proton and electric potential gradient that is generated between the two sides of the photosynthetic membrane, because the electron transport is accompanied by a proton transport from the periplasm to the cytoplasm. Protons flowing back along the gradient through the channel of membrane spanning ATPase can drive chemical energy storage through phosphorylation of ADP to ATP (cf. Fig. 2.14). In plants, there are two types of photosynthetic reaction centers. The photoelectron transfer chain from reaction center I leads to the reduction of the $NADP^+$. The oxidized special pair in reaction center I is reduced at the end of the photoelectron transfer chain from reaction center II, which in turn recovers its electron by the oxidation of water, mediated by a close-by manganese complex and leading to the generation of molecular oxygen.

2.2.2 Excited State Proton Transfer Reactions

Electronically excited states behave differently from the ground state because the distribution of electron density over the atoms in a molecule is changed. As was shown in the last section, this goes along with a change in the effective redox-potential, leading to stronger oxidation and reduction power. Likewise, the ability

to accept or donate protons is changed upon electronic excitation. This effect can be measured by the change of the acid dissociation constant K_a, usually expressed by the pK_a value:

$$pK_a = -\log K_a \tag{2.20}$$

For excited states, the pK_a is usually denoted with an asterisk, i.e., as pK_a*. As an example, the case of 2-naphthol is shown in Fig. 2.24. In a diagram representing the fractions of undissociated (acid) and dissociated (basic) form as a function of *pH*, the pK_a value can be read from the point where both forms are present in equal amounts. In the ground state, 2-naphthol exhibits a pK_a of 9.2, i.e., it is a rather weak acid. In the first excited singlet state the pK_a* jumps up to a value of 2, i.e., the compound turns to a fairly strong acid. The reason for this, is a shift of electron density away from the oxygen atom to the aromatic ring system when an electron is excited from the LUMO to the HOMO.

Proteolytic processes in the excited singlet state can be easily monitored by fluorescence spectroscopy. If a molecule is excited, for example at a pH where the acidic form prevails in the ground state, but the fluorescence observed is specific to the basic form, this means that a deprotonation of the excited acidic form must have taken place during its excited state lifetime. Furthermore, this is evidence of the fact that the system remains on the excited state potential surface during the reaction and thus represents an example of an adiabatic photoreaction. In Fig. 2.25, the situation is illustrated for 2-naphthol. The position of the equilibrium between the acidic (neutral, protonated) and the basic (anionic, deprotonated) form at a particular *pH* can be judged from the absorption spectra. At *pH* values greater than 8, changes toward the shape of the final spectrum associated with the basic form become clearly visible. (cf. left-hand side of Fig. 2.25). The fluorescence spectra on the right-hand side of Fig. 2.25 were taken at delay times of several

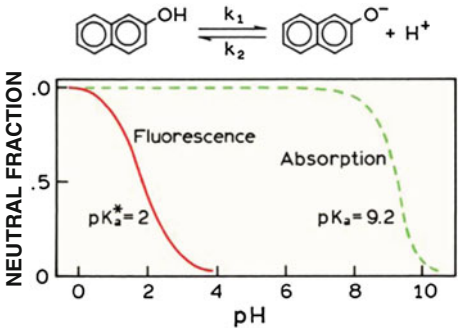

Fig. 2.24 pH-dependence of proteolytic dissociation equilibrium of 2-naphthol in the ground and in the excited singlet state. Reprinted with permission from Fig. 7.43 in Ref. [4], Lakowicz JR, Principles of fluorescence spectroscopy. Third Edition. Springer Science+Business Media, Copyright © 2006, 1999, 1983 Springer Science+Business Media, LLC, with kind permission from Springer Science+Business Media B.V

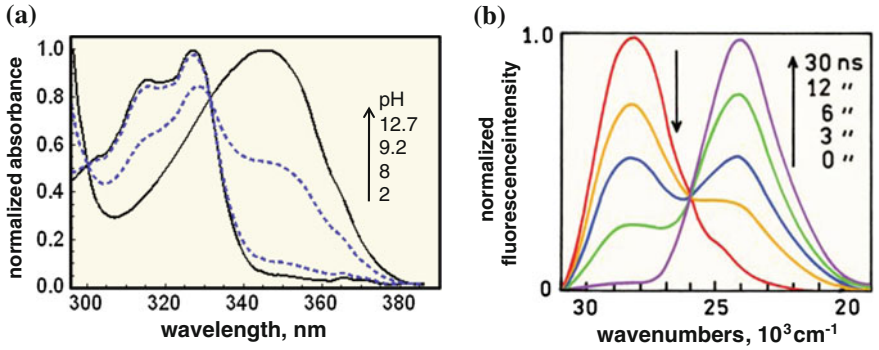

Fig. 2.25 *Left*: absorption spectra of 2-naphthol at various *pH* values *Right*: fluorescence spectra recorded in solutions of *pH* 6.6 at various delay times after a short laser pulse. The spectra are corrected for the intensity decrease due to the decay of the excited state population. *Left*: adapted from Fig. 7.42, *right*: reproduced from Fig. 7.47 in Ref. [4], Lakowicz JR, Principles of fluorescence spectroscopy. Third Edtion. Springer Science+Business Media, Copyright © 2006, 1999, 1983 Springer Science+Business Media, LLC, with kind permission from Springer Science+Business Media B.V

nanoseconds after a short excitation pulse at a *pH* of 6.6. At this *pH*, the molecule in its ground state equilibrium is still completely undissociated. Immediately after excitation, the fluorescence spectrum corresponds to the mirror image of the absorption band of the acidic form, but then it is gradually converted to a band at longer wavelength, characteristic of the 2-naphtholate anion. This observation reflects the time scale of the deprotonation process.

The fluorescence observations accompanying proteolytic equilibria in the excited state were first explained by Förster, who suggested the spectroscopic/thermodynamic cycle, the so-called Förster cycle, represented in Fig. 2.26. From the cycle and the principle of conservation of energy, spectroscopic and thermodynamic energies can be combined and lead to the following relation:

$$pK_a^* - pK_a = \frac{E_{A^-} - E_{HA}}{2.3\,RT} \tag{2.21}$$

It allows to estimate the pK_a* value from the spectroscopic energies E_{A^-} and E_{AH} of the basic and the acidic form, respectively. These energies can be taken either from the absorption spectra or from the fluorescence spectra. As follows qualitatively from Eq. (2.21), the excited state is more acidic (has a lower pK_a* value) than the ground state, if the absorption (or the emission) of the basic form is at lower energy (longer wavelength) than of the acidic form. This is usually the case for neutral acids (cf. the naphthol case shown in Fig. 2.25). The opposite is generally true if the basic from is neutral, e.g., in aromatic amines.

Excited state proton transfer reactions can be also found in natural systems. A prominent example is the emission of the green fluorescent protein [27] that has acquired great significance because it can be genetically engineered and

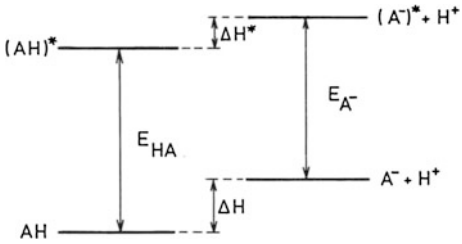

Fig. 2.26 Scheme of the Förster cycle relating spectral and thermodynamic quantities for proton transfer in ground and excited states. Reprinted with permission from Ref. [26], Marciniak B, Kozubek H, Paszyc S (1992) *Journal of Chemical Education*, Vol. 69, No. 3, 1992, pp. 247–249. Copyright © 1992, Division of Chemical Education Inc

implemented as a fluorescence marker to study cell biological problems in many organisms. The fluorescent chromophore is shown in Fig. 2.27. In the ground state, the phenolic OH group is undissociated, although part of a hydrogen bonded network of various amino acids. On excitation, a proton transfer takes place along this network and the emission arising is characteristic of the anionic, i.e., deprotonated chromophore.

2.2.3 Photochemical Cis/Trans-Isomerizations

Whereas, internal molecular rotations around single bonds between carbon and heteroatoms are fairly and easily achieved, internal rotations around double bonds are hindered by high activation barriers. Such barriers arise from the decreasing overlap of the vicinal p_π-orbitals as the π-plane of the neighboring centers adopts a perpendicular configuration. In Fig. 2.27, the energetic effect of such a rotation on the energy of the π-molecular orbitals is schematically shown for the case of ethylene. During the rotation, the energies of HOMO and LUMO approach each other. At 90°, i.e., in the perpendicular configuration, both orbitals become

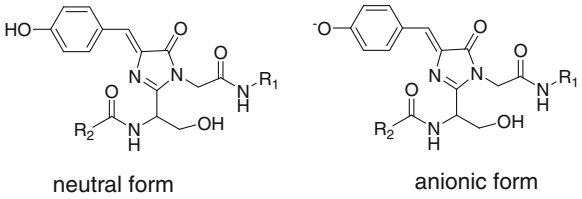

Fig. 2.27 Fluorescent chromophore of the green fluorescent protein. R_1 and R_2 represent the continuation of the protein chain, wherein the chromophore was formed from a serine/tyrosine/glycine motif. On excitation to the S_1 state, the neutral form is rapidly deprotonated and emits the fluorescence specific of the anionic form

degenerate and are nonbonding. Continuing the rotation to 180° HOMO and LUMO are interchanged as compared to the situation at the beginning. Thus, considering the state energy of the electronic configurations with both π-electrons in the HOMO, the ground state, would be raised up to the energy of S_2 (in that simple picture) after rotation by 180°. The first excited singlet, corresponding to an electron configuration with one electron in the HOMO and one in the LUMO, would keep its energy unchanged on such a rotation, and the S_2 state, with both electrons in the LUMO in the beginning, would end up as S_0 after a 180° rotation. Although this description is rather simplified, it conveys the essential concept and demonstrates the electronic origin of the potential curves in the ground and excited states.

A representation of the S_1 and S_2 potential surfaces of stilbene versus two relevant coordinates as calculated by a full ab initio quantum chemical calculation is also shown in Fig. 2.28. From it, the dynamics of a molecule after excitation to the excited state may be anticipated. After exciting the molecule in its *trans*-conformation ($\phi = 180°$) it finds itself on a very flat surface and will eventually proceed toward the perpendicular ($\phi = 90°$) conformation where the potential surface exhibits a minimum. Upon radiationless deactivation to the lower potential surface of the ground state, the molecule will end up on a potential hill and may proceed further to the right or to the left, i.e., toward the *cis*-conformation or back

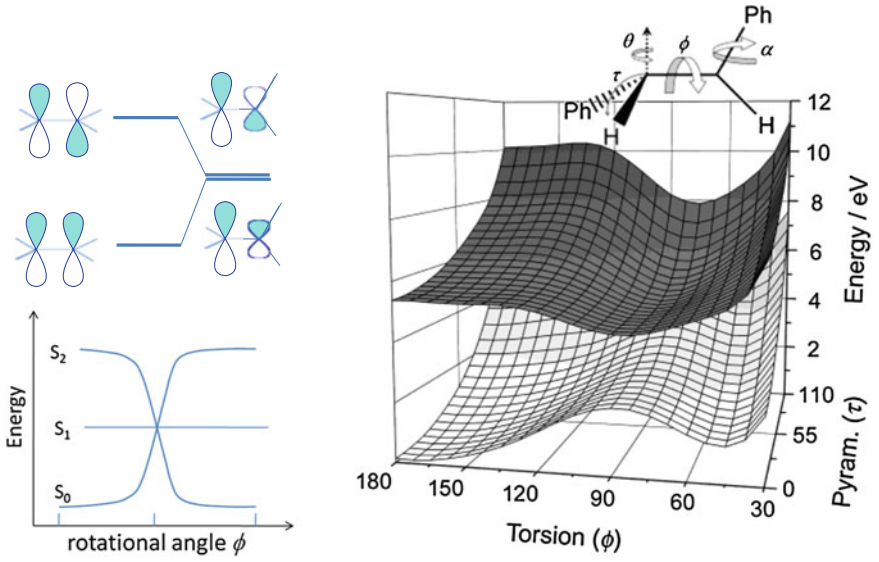

Fig. 2.28 *Left*, *top*: effect of of C–C bond rotation angle ϕ on π orbitals and energy scheme of ethylene. *Left*, *bottom*: schematic energy dependence for different configurations of two electrons in the MO scheme above. *Right*: quantum chemical potential surfaces for S_o and S_1 of stilbene along the coordinates ϕ of C–C bond rotation and τ of pyramidal distortion as defined in the figure. *Right*-hand side reprinted with permission from Ref [28]., Quenneville J, Martínez TJ J Phys Chem A 107:829–837, Copyright © 2003, American Chemical Society

to the *trans*-conformation. Experimentally, it is indeed found that the quantum yields from *trans* to *cis* or from *cis* to *trans* are both on the order of 50 % [29]. It must be mentioned, though, that the real mechanism of this photoreaction may be much more complex and may involve the potential surface of the excited triplet state, too, as well as distortions of additional motional degrees of freedom such as the pyramidal distortion indicated in Fig. 2.28 as points of transition between different potential surfaces.

Whereas, for C=C double bonds, rotation around the bond is the only way to achieve the *cis/trans*-isomerization, there are other options in the case of double bonds involving heteroatoms. A much studied system is azobenzene which is used as a chemical actinometer and is a very prominent candidate in modern research about molecular devices. Here the photoisomerization process implies a rehybridization at one of the nitrogen atoms with an intermediate linearization of the N=N–C angle [30, 31] (Fig. 2.29).

In nature, *cis/trans*-photoisomerization provides the mechanism of two important biological functions. The first is the process of vision where the key chromophore is the polyene retinal, chemically bound through a azomethine function (Schiff base) to the protein opsin to form the rhodopsin unit, which is to be found in the light sensitive cells of the retina [32]. In the dark, the retinylidene group is in an 11-*cis* configuration (cf. Fig. 2.30). It isomerizes to the all-*trans* form upon light excitation. This process triggers a sequence of events during which the retinal is released and new rhodopsin is generated by the binding of fresh 11-*cis* retinal to the opsin.

The *cis/trans*-photoisomerization of rhodopsin serves another important function in photosynthetic archaea as *halobacterium halobium,* a single-celled microorganism that stands extreme habitats such as hot springs and salt lakes. Here the dark state of the retinylidene moiety is all-*trans* (cf. Fig. 2.30) and undergoes a *trans* to *cis* photoisomerization of the double bond at position 13 upon which a proton at the azomethine nitrogen atom is released. Again, this process is part of a cycle, which, in this case, however, does not elicit a nerve signal but serves to pump protons across the cell membrane, so that a proton gradient between inner and outer space of the membrane is created [33]. Thus, the light energy is transformed to osmotic energy and later to chemical energy via the transformation of ADP to ATP.

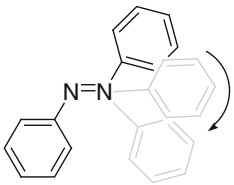

Fig. 2.29 Photoisomerization pathway of azobenzene

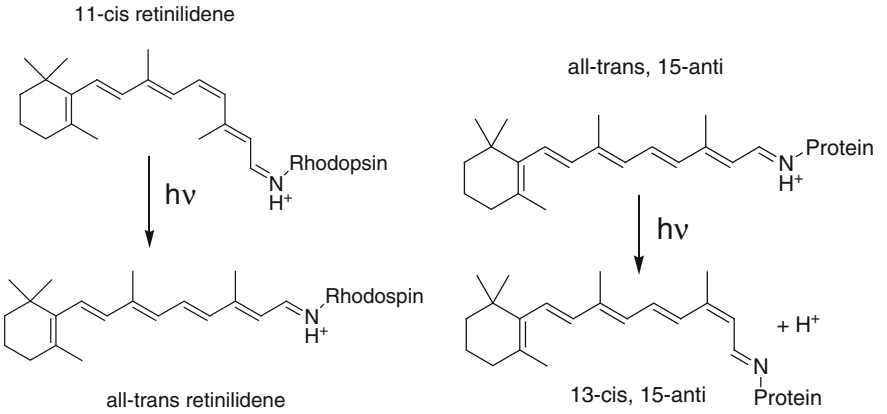

Fig. 2.30 *Left*: Primary photochemical process in vision. *Right*: Primary photochemical process of light-driven proton pump involving bacteriorhodopsin in halobacteria

References

1. Parson WW (2007) Modern optical spectroscopy. With exercises and examples from biophysics and biochemistry. Springer, Berlin Heidelberg
2. Burgess C, Frost T (eds) (1999) Standards and best practice in absorption spectrometry. Blackwell Science, London
3. Gore MG (ed) (2000) Spectrophotometry & Spectrofluorimetry. Oxford University Press, Oxford
4. Lakowicz JR (2006) Principles of fluorescence spectroscopy. Springer Science+Business Media, New York
5. Schweitzer C, Schmidt R (2003) Physical mechanisms of generation and deactivation of singlet oxygen. Chem Rev 103(5):1685–1757
6. Turro NJ, Scaiano JC, Ramamurthy V (2009) Principles of molecular photochemistry: an introduction. University Science Books, Sausalito
7. Klán P, Wirz J (2009) Photochemistry of organic compounds. From concept to practice. Wiley, Chichester
8. Stochel G, Brindell M, Macyk W, Stasicka Z, Szacilowski K (2009) Bioinorganic photochemistry. Wiley, Chichester
9. Kavarnos GJ (1993) Fundamentals of photoinduced electron transfer. VCH Publishers, New York
10. Kohen E, Hirschberg J, Santus R (1995) Photobiology. Academic Press, San Diego
11. Batschauer A (ed) (2003) Photoreceptors and light signalling. Comprehensive series in photochemical and photobiological sciences. The Royal Society of Chemistry, Cambridge
12. Schmidt W (2000) Optische spektroskopie. Wiley-VCH, Weinheim
13. Murrell JN (1963) The theory of the electronic spectra of organic molecules. Methuen&Co, London
14. Byron CM, Werner TC (1991) Experiments in synchronous fluorescence spectroscopy for the undergraduate instrumental chemistry course. J Chem Educ 68:433–436
15. Diez M, Zimmermann B, Börsch M, König M, Schweinberger E, Steigmüller S, Reuter R, Felekyan S, Kudryavtsev V, Seidel CAM, Gräber P (2004) Proton-powered subunit rotation in single membrane-bound F_0F_1-ATP synthase. Nat Struct Mol Biol 11:135–141

16. Schmidt R (2006) Quantitative determination of $^1S_g^+$ and ^1D_g singlet oxygen in solvents of very different polarity. General energy gap law for rate constants of electronic energy transfer to and from O_2 in the absence of charge transfer interactions. J Phys Chem A 110:2622–2628
17. Bodesheim M, Schütz M, Schmidt R (1994) Triplet state energy dependence of the competitive formation of O_2 ($^1S_g^+$), O_2 (^1D_g) and O_2 ($^3S_g^-$) in the sensitization of O_2 by triplet states. Chem Phys Lett 221:7–14
18. Schmidt R (2006) The effect of solvent polarity on the balance between charge transfer and non-charge transfer pathways in the sensitization of singlet oxygen by pp* triplet states. J Phys Chem A 110(18):5990–5997
19. Förster T (1970) Diabatic and adiabatic processes in photochemistry. Pure Appl Chem 24:443–449
20. Miller JR, Calcaterra LT, Closs GL (1984) Intramolecular long-distance electron transfer in radical anions. The effect of free energy and solvent on reaction rates. J Am Chem Soc 106:3047–3049
21. Marcus RA (1956) On the theory of oxidation-reduction reactions involving electron transfer. I. J Chem Phys 24:966–978
22. Marcus RA (1956) Electrostatic free energy and other properties of states having nonequilibrium polarization. I J Chem Phys 24:979–989
23. Marcus RA (1957) On the theory of oxidation-reduction reactions involving electron transfer. III. Applications to data on the rates of organic redox reactions. J Chem Phys 26:872–877
24. Degtyarenko KN, North ACT, Findlay JBC (1999) PROMISE: a database of bioinorganic motifs. Nucleic Acids Res 27:233–236
25. Deisenhofer J, Michel H (1992) High-resolution crystal structures of bacterial photosynthesis reaction centers. In: Ernster L (ed) Molecular mechanisms in bioenergetics. Elsevier, Amsterdam, pp 103–120
26. Marciniak B, Kozubek H, Paszyc S (1992) Estimation of pK_a* in the first excited singlet state. J Chem Educ 69:247–249
27. Tsien RY (1998) The green fluorescent protein. Annu Rev Biochem 67:509–544
28. Quenneville J, Martínez TJ (2003) Ab initio study of cis-trans photoisomerization in stilbene and ethylene. J Phys Chem A 107:829–837
29. Gegiou D, Muszkat KA, Fischer E (1968) Temperature dependence of photoisomerization. V. The effect of substituents on the photoisomerization of stilbenes and azobenzenes. J Am Chem Soc 90:3907–3918
30. Rau H, Lüddecke E (1982) On the rotation-inversion controversy on photoisomerization of azobenzenes. Experimental proof of inversion. J Am Chem Soc 104:1616–1620
31. Rau H (1984) Further evidence for rotation in the pp* and inversion in the np* photoisomerization of azobenzenes. J Photochem 26:221–225
32. Stuart JA, Brige RR (1996) Characterization of the primary photochemical events in bacteriorhodopsin and rhodopsin. In: Lee AG (ed) Rhodopsin and G-protein linked receptors, part A, vol 2. JAI Press, Greenwhich, Conn, pp 33–140
33. Haupts U, Haupts C, Oesterhelt D (1995) The photoreceptor sensory rhodopsin I as a two-photon-driven proton pump. Proc Natl Acad Sci 92:3834–3838

http://www.springer.com/978-3-642-39628-1

Photodynamic Therapy
From Theory to Application
Abdel-Kader, M.H. (Ed.)
2014, XX, 312 p. 184 illus., 142 illus. in color.,
Hardcover
ISBN: 978-3-642-39628-1